

Effects of Materials Parameters and Design Details on the Fatigue of Composite Materials for Wind Turbine Blades

John F. Mandell and
 Daniel D. Samborsky
 Dept. of Chemical Engineering
 Montana State University
 Bozeman, MT, USA 59717
 Phone: (406) 994-4543
 FAX: (406) 994-5308
 e-mail: johnm@coe.montana.edu

Herbert J. Sutherland*
 Wind Energy Technology Dept.
 Sandia National Laboratories[†]
 MS-0708
 Albuquerque, NM, USA 87185
 Phone: (505) 844-2037
 FAX: (505) 845-9500
 e-mail: hjsuthe@sandia.gov

ABSTRACT: This paper presents an analysis of the results of nine years of fatigue testing represented in the U.S. Department of Energy / Montana State University (DOE/MSU) Composite Materials Fatigue Database. The focus of the program has been to explore a broad range of glass-fiber-based materials parameters encompassing over 4500 data points for 130 materials systems. Significant trends and transitions in fatigue resistance are shown as the fiber content and fabric architecture are varied. The effects of structural details including ply drops, bonded stiffeners, and other geometries that produce local variations in fiber packing and geometry are also described. Fatigue tests on composite beam structures are then discussed; these show generally good correlation with coupon fatigue data in the database. Goodman diagrams for fatigue design are presented, and their application to predicting the service lifetime of blades is described.

Keywords: Composites, Fatigue, Data Bases, Fiber Reinforced Plastics (FRP)

1. INTRODUCTION

There are two main fiberglass composite databases for wind turbine applications. The first is the DOE/MSU database that has been developed in the U.S. by Mandell et al. [1], and the second is the European database. The latter is a compilation of the work of many researchers, which has been compiled as the FACT database by de Smet and Bach [2]. The European database is best characterized as the study of a few materials in great depth, and the former is best characterized as the study of many materials in not as much depth. The two databases are in general agreement as to trends in fiberglass fatigue behavior, the major differences are in compression fatigue. This paper provides an overview of the significant trends in fatigue behavior from the DOE/MSU database in terms of materials parameters and application to composite structures [1, 3-10]. Sutherland [11] presents an overview of these results as well as other considerations in the general fatigue analysis of wind turbines.

The fatigue data presented here were obtained from constant stress amplitude tests at a fixed R value, where R is the ratio of the minimum stress to the maximum stress. Test details can be found in Mandell and Samborsky [1]. The S-N fatigue data trends for maximum stress, σ , vs. cycles to failure, N, are commonly represented as linear on either a log-linear or log-log basis. The former takes the form

$$\sigma/\sigma_0 = C / b \log N \quad (1)$$

where σ_0 is the single-cycle ultimate strength and C typically has a value close to 1.0; b is then the slope of the S-N curve, termed the "fatigue coefficient". The log-log representation takes the form

$$\sigma/\sigma_0 = C N^{1/m} \quad (2)$$

where C often differs substantially from 1.0, and m is the "fatigue exponent" related to fatigue crack growth [1,12, 13]. Data sets for different laminates tend to fit better to one or the other of Eqs. (1) or (2). The representation used in most of this paper is Eq. (1), with Eq. (2) used to reduce high cycle data for Goodman Diagrams for design, due to a better fit to that particular data set. Thus, most of the discussion will center on the fatigue coefficient, b, in Eq. (1); a higher coefficient represents a steeper S-N curve, ie, increased fatigue sensitivity.

Most of the data in the DOE/MSU database are presented in terms of maximum initial strain measured in the early cycles of the test (strain values are obtained by dividing the stress by the modulus). The maximum initial strain that produces a lifetime of 10^6 cycles is also used as a convenient basis for comparing materials. For a wind turbine blade having a particular section stiffness distribution, it is the strain capability of the material in fatigue that is of greatest interest.

2. EFFECTS OF MATERIALS PARAMETERS

2.1 Overall Data Trends

A sampling of data points from different materials in the DOE/MSU database is plotted in Fig. 1. These data are for fiberglass composites with at least 25 percent fiber in the loading direction, tested at R=0.1. When fit with Eq. (1), the "good" materials have a fatigue coefficient, b, of 0.10 and the "poor" have a value of 0.14. The good materials in this figure are approaching the best fatigue behavior that can be obtained for fiberglass materials in

* Author to whom correspondence should be addressed.

† Sandia is a multiprogram laboratory operated by Sandia Corporation, a Lockheed Martin company, for the U.S. Department of Energy under contract DE-AC04-94AL85000.

Disclaimer

This report was prepared as an account of work sponsored by an agency of the United States Government. Neither the United States Government nor any agency thereof, nor any of their employees, makes any warranty, express or implied, or assumes any legal liability or responsibility for the accuracy, completeness, or usefulness of any information, apparatus, product, or process disclosed, or represents that its use would not infringe privately owed rights. Reference herein to any specific commercial product, process, or service by trade name, trademark, manufacturer, or otherwise does not necessarily constitute or imply its endorsement, recommendation, or favoring by the United States Government or any agency thereof. The views and opinions of authors expressed herein do not necessarily state or reflect those of the United States Government or any agency thereof.

DISCLAIMER

Portions of this document may be illegible in electronic image products. Images are produced from the best available original document.

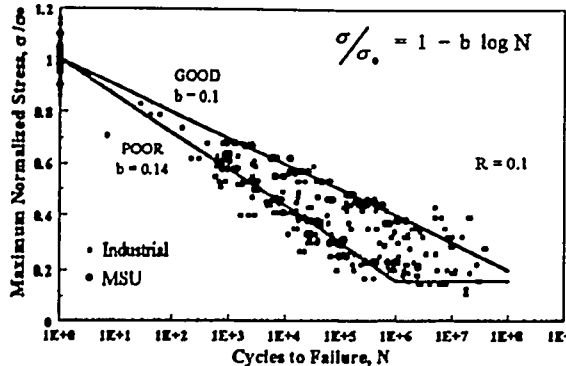


Figure 1. Extremes of Normalized S-N Tensile Fatigue Data for Fiberglass Laminates, $R = 0.1$ [1].

tensile fatigue (the 10% rule: uniaxial fiberglass composites at $R = 0.1$) [1, 12], while the poor materials do not perform nearly as well. Indeed, the apparently small variation in b is indicative of significant differences in fatigue performance. As shown in the figure, at 20% of static strength, the good materials have almost 2.5 orders of magnitude longer life than the poor materials. As reported by Mandell and Samborsky [1], for compressive fatigue, the good materials have a b of 0.07, and the poor materials have a b of 0.11. For reverse fatigue, the values of b are 0.12 and 0.18, respectively. The range of values in compression fatigue is lower than in tensile fatigue and shows much less sensitivity to materials parameters. The following discussion breaks out the effects of particular materials parameters included in Fig. 1 for tensile fatigue, $R=0.1$.

2.2 Fiber Content

Glass fiber composites have long been recognized as having inferior fatigue resistance compared to carbon fibers [12]. It has also been recognized that many woven glass-fabric composites show even poorer tensile fatigue resistance than the well-aligned, uniformly dispersed systems [12]. Typical reinforcing fabrics used in wind turbine blades have either stitched or woven strand structures (Fig. 2), so that the individual fibers are not uniformly dispersed in the matrix.

One of the most significant and surprising findings of the test program [1] is that the tensile fatigue performance of all stranded fabric materials systems tested become much less fatigue resistant as the overall fiber volume content increases beyond the range of 35-45%. The behavior changes from "good" to "poor" in Fig. 1 as the fiber content increases. At the same time, the maximum strain that can be withstood for 10^6 cycles drops from the 1.0 to 1.2% range down to the 0.4 to 0.8% range [1].

Figure 3 shows this trend for a particular composite system containing the D155 (0°) and DB120 ($\pm 45^\circ$) fabrics in the configuration [0/ $\pm 45/0$], containing 72% 0° material and 28% $\pm 45^\circ$ material. The extremes of "good" and "poor" performance in Fig. 1 are achieved simply by varying the overall fiber content. Fig. 4 (a) represents these data in terms of the fatigue coefficient, b , vs. the fiber content, showing a transition to poor behavior as the fiber content increases above 42% fibers by volume. Also shown are data for a "triax" fabric system which produces "poor" results even at low fiber contents, as discussed later. The 42% fiber content is typical of the upper range achieved in

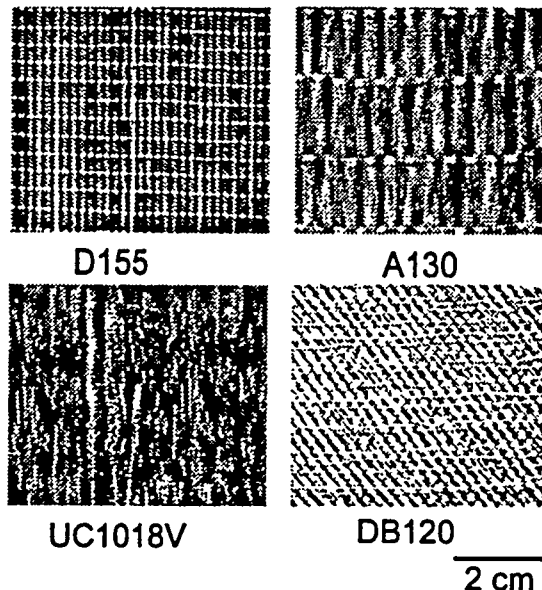


Figure 2. Dry Fabric Samples [10].

hand layup manufacturing, and the lower range for processes including pultrusion and resin transfer molding (RTM). (For consistency, all materials presented after Fig. 1 were obtained using RTM). Fig. 4(b) presents similar data for unidirectional (all 0°) composites fabricated from the stitched D155 fabric as well as a lighter-weight D092 fabric and the woven A130 fabric shown in Fig. 2. The trend is similar to laminates including $\pm 45^\circ$ plies, but is shifted to a slightly higher fiber content. When the stitching is removed from the D155 fabric, the fatigue resistance is greater at higher fiber contents.

The origin of the sharp decrease in fatigue resistance as the fiber content increases apparently lies in a transition to a condition where the laminate fails in fatigue soon after the matrix cracks, usually along the stitching or weave cross-over [1]. When 45° plies are present, poor performance is observed if the 0° plies fail soon after the $\pm 45^\circ$ plies form matrix cracks. "Good" performance is associated with the 0° fiber wearing-out gradually, as occurs in the testing of a single strand of material [1, 12].

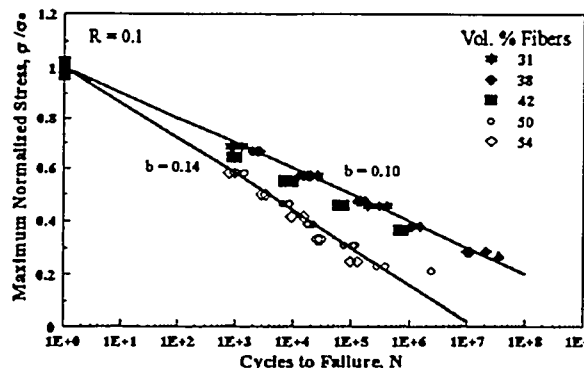


Figure 3. Normalized S-N Fatigue Data at Various Fiber Contents for a Single Family of Fiberglass Laminates with 72% 0° Plies and 28% $\pm 45^\circ$ Plies, $R = 0.1$ [1].

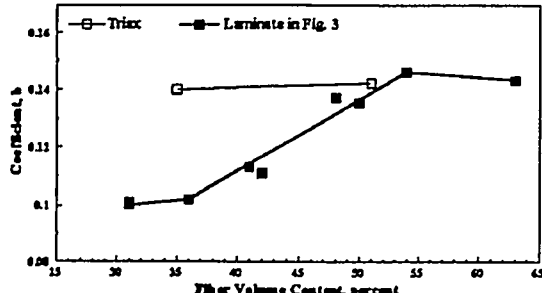


Figure 4(a). Laminates with 0° and $\pm 45^\circ$ Plies.

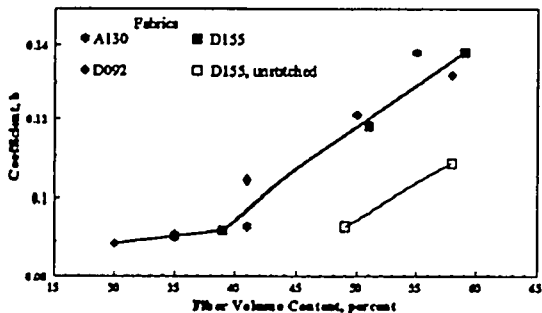


Figure 4(b). Unidirectional Fiberglass Laminates.

Figure 4. Fatigue Sensitivity Coefficient for Fiberglass Laminates as a Function of Fiber Content, at $R = 0.1$ [1].

Detailed finite element analysis [1, 5] has shown that a layer of matrix between the fibers of adjacent plies greatly reduces the concentration of stress in the 0° strands near points of matrix cracking in adjacent plies. As the fiber content increases, the tight strands in many fabrics are forced together, leading to matrix crack induced premature failure in tensile fatigue. Similarly, the crowding of strands in certain structural details such as ply-drops can lead to the same problem, as discussed later.

2.3 Fabric Architecture

The geometry of reinforcing fabrics plays a major role in static and fatigue properties. Samborsky et al [9] gives a comparison of static and fatigue properties for several types of E-glass fabric laminates used for the 0° plies. Ultimate tensile strength and elastic modulus are relatively insensitive to fabric type, but ultimate compressive strength is significantly lower for fabrics like A130 with a weave geometry that produces an out-of-plane curvature to the strands. Woven fabrics have about half the compressive strength of fabrics with straight strands. As noted earlier, the compressive fatigue resistance, when normalized by the ultimate compressive strength, is insensitive to fabric type or fiber content [1]. (It should be noted that the straight-strand fabrics will also have significantly reduced compressive strength if the fibers become "wavy" during fabrication.)

The tensile fatigue resistance is particularly poor for "triax" fabric laminates, where the 0° and $\pm 45^\circ$ layers are stitched together. As indicated in Fig. 4(a), the triax has "poor" tensile fatigue resistance even at low fiber contents typical of hand layup. When the 0° plies are separated from the $\pm 45^\circ$ plies, as in the [0/ ± 45 /0], laminates in Fig. 4(a), the tensile fatigue resistance can be "good" at low fiber

contents, but becomes "poor" as the fiber content increases, as discussed earlier. Several other triax fabrics have been tested with similar (or worse) findings [1]. Fabrics like A130, with somewhat looser strands than the D155 in Fig. 4(a), perform better at higher fiber contents. Recent data [9] for the bonded fabric UC1018V also show improved performance at high fiber content due to the absence of tight strands (similar results are given in Fig. 4(b) for D155 with stitching removed). However, it is not necessarily true that all unidirectional fabrics like D155 (a weft-direction fabric: fibers perpendicular to the fabric roll), show good tensile fatigue resistance at low fiber contents. This is the case with the warp direction fabric A1010, similar to D155. A1010 gave relatively "poor" tensile fatigue performance at low fiber content, apparently due to differing details of the stitch pattern [10].

2.4 Relative Amount of 0° Plies

The skins and webs of wind turbine blades are often composed of laminates with a relatively high content of $\pm 45^\circ$ plies, while the main structure usually contains a high content of 0° plies. Mandell and Samborsky [1] provides data for laminates with a wide range of 0° vs. $\pm 45^\circ$ ply content. These data also cover a range of fiber contents. Laminates with high $\pm 45^\circ$ ply contents fail in fatigue at lower strains than do laminates with high 0° ply contents [1]. Laminates with 20% to 40% 0° material show a similar trend in fatigue coefficient, b , to the 72% 0° laminate in Fig. 4(a), but the transition to a higher value of b is shifted to 3 to 5% lower fiber content [1].

2.5 Matrix and Fiber Materials

The matrix material in laminates with typical (relatively brittle) polyester, vinylester, and epoxy matrices has little effect on the static or fatigue properties (tension and compression) in the 0° direction of laminates with a high 0° content [1]. However, tougher, more ductile versions of these matrices may produce greater transverse direction and interlaminar properties. The heat and moisture resistance is also matrix dependent. Tougher matrices are a topic of current research, the results of which will appear in the DOE/MSU database.

Carbon fibers are known to provide much greater tensile fatigue resistance in the fiber direction as compared to glass fibers [12]. Normalized tensile fatigue resistance in directions other than 0°, and in compression in all directions, is matrix dominated, and is insensitive to the fiber type, although working strain levels may be reduced by the higher modulus of carbon fibers.

3. STRUCTURAL DETAILS AND SUBSTRUCTURE

3.1 Structural Details

The extension of coupon data to the behavior of full-sized structural components is being studied using such details as ply drops, adhesive bonds, molded-in surface indentations and transverse cracks [1, 7-9]. The results of the studies are summarized in Table 1, where the "knock-down" factor F is defined to be the ratio of the maximum cyclic strain of a uniform coupon to that of a structured coupon at one million (10^6) cycles; namely:

Table 1. Knock-Down Factors for Tension and Compression. Laminates with Approximately 70% 0° material. Based on D155, A130 and UC1018V Fabrics [1,9].

Detail	Sketch	Knock-Down Factor, F		
		A130 fabric	D155 fabric	UC1018V fabric
Simple Coupon (Straight Material)		1.0	1.0	1.0
Surface Indentation Tension, R = 0.1 (Vf increased, thickness reduced by 25%)		1.6	2.5	1.7
Surface Indentation Compression, R = 10 (Vf increased, thickness reduced by 25%)		1.0	1.4	—
Locally Higher Fiber Content (2 - 90 plies in center) Tension, R = 0.1		2.1	1.5	—
Locally Higher Fiber Content (2 - 90 plies in center) Compression, R = 10		1.0	1.4	—
Exterior Cracked Transverse 90° Patch, R = 0.1		—	1.0	—
Double Interior 0° Ply Drop R = 0.1		1.4	1.6	—

$$F = \frac{\text{Uniform Coupon Maximum Strain} @ 10^6 \text{ Cycles}}{\text{Structured Coupon Maximum Strain} @ 10^6 \text{ Cycles}} \quad (3)$$

One common feature of blade structures is the use of ply drops to tailor the thickness of the composite structure to meet loads criteria while minimizing weight. Several configurations for the ply drops have been experimentally investigated and analyzed in terms of delamination growth under tensile and fatigue loading [7]. The ply drop may be internal (covered by at least one layer of fabric) or external. The external ply drop is significantly more susceptible to delamination than an internal ply drop and is not recommended as a good design practice; single ply drops also perform better than multiple drops at the same position; ply drops should be spaced at least 25mm apart. As shown in Table 1, ply drops also create local stress concentrations that can significantly reduce fatigue lifetimes. For the same ply drops, thicker laminates are better in resisting delaminations. As measured in an increased knock-down factor [8], dropping two plies in the same location is twice as harmful as dropping a single ply.

As discussed above, the fiberglass laminates typically used in wind turbine blades are susceptible to significant degradation in their fatigue properties if fibers are forced very close to one another. The effect is noted in the dependence of the fatigue coefficient on fiber density shown in Fig. 4. This effect also translates into local manufacturing defects, simulated by surface indentations and excess fiber layers. As shown in Table 1 for D155 fabric, a surface indentation produces a knock-down factor of 2.5 for a local increase in fiber content from 36% to 52%, and excess layers produce a knock-down factor of 1.5 for a local increase in the fiber volume from 35% to 47%.

In typical layups for composite structures, and especially for wind turbine blades, a high percent of the

fibers are aligned with the primary load direction. Additional off-axis layers are added to prevent splitting and to increase shear properties. As discussed above, these off-axis layers are typically more susceptible to fatigue damage. The designer would hope that these layers would split off from the underlying layers that carry the main loads without causing them to fail prematurely. Thus, Table 1 indicates that no knock-down factor is required for the propagation of transverse cracks into typical laminates. This is based on the assumption that fiber separation is adequate to prevent the fiber density effects discussed above. The structural detail effects discussed here are based on low fiber content laminates that follow the "good" behavior in Fig. 1. Limited data indicate that structural details have a reduced effect on initially "poor" laminates. In particular, woven fabrics under compressive fatigue have poorer performance in the base laminate as compared to straight strands (un-normalized data), but the knock-down factor is significantly reduced in structural details (Table 1).

3.2 Substructure Studies

In a related study [10], the static and fatigue behavior of I-beam substructural elements has been investigated using a variety of materials from the DOE/MSU database [1]. The beams are intended to represent typical substructures of blades. Figure 5 shows the geometry of the heavily shear-stiffened beams loaded in four-point bending. The beams were RTM molded in parts, then secondary-bonded as shown. The beam stiffness and strains were well-predicted by finite element analysis, as discussed in detail in Mandell et al [10].

Beams fabricated with flanges which behaved "poorly" in tensile fatigue (Fig. 1) failed on the tensile flange in fatigue, with a compressive flange failure in static tests. Figure 6 gives a comparison of flange material coupon and beam failure strain data for this series using "triax" fabric flange laminates. The beam failure conditions are in good agreement with the coupon fatigue data for both strains and cycles at failure and failure mode.

When beams were fabricated with "good" tensile fatigue laminates (Fig. 1), the strain performance of the beams was improved, compared to the data in Fig. 6. However, the failure mode in the beams was now more complex, in many cases involving initial failure in the web flange layer adjacent to the flange, with subsequent flange

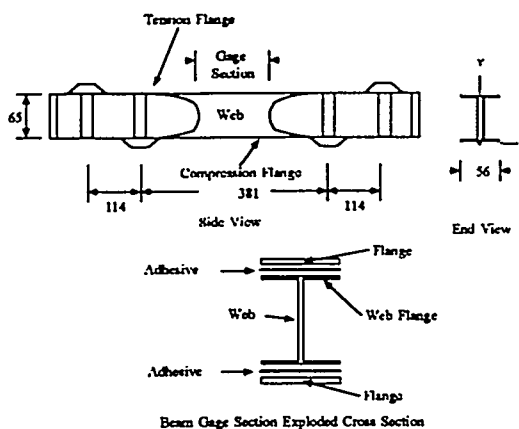


Figure 5. Beam Geometry (Dimensions in mm).

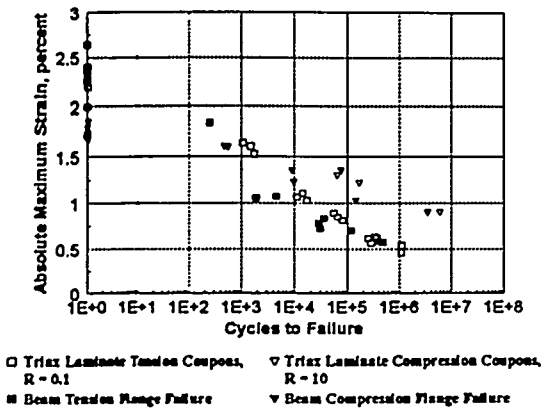


Figure 6. Beams with Triax Laminate Flanges and $\pm 45^\circ$ web. Comparison of Flange Coupon Data with Beam Data [11].

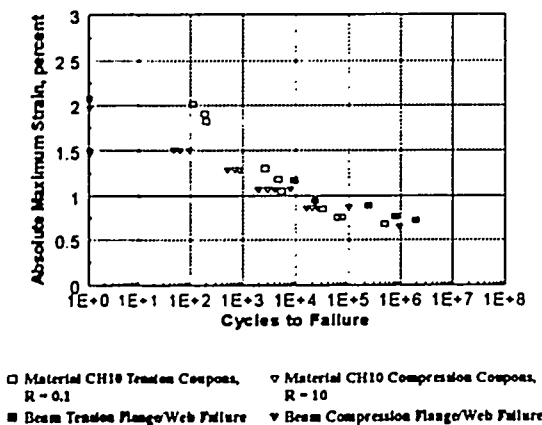


Figure 7. Beams with 72% 0° Flanges and $\pm 45^\circ$ Web. Comparison of Web Coupon Data to Beam Data [11].

delamination [10]. This failure mode was predictable, based on the materials used for the web, which contained all $\pm 45^\circ$ plies. Figure 7 gives data for beams with 72% 0° flanges and all $\pm 45^\circ$ material in the web. Compared to the web coupon fatigue data shown, the beam results are in good agreement (here, the beam outside flange strains are reduced to reflect the position of the web flange). Compared with the flange coupon data, the beam strain data are somewhat low (see Mandell et al [10]). Efforts to improve the web performance by adding more 0° material produced no significant improvement in beam strain to failure in fatigue, as the failure mode became dominated by delamination in the adhesive.

The beam study showed that the materials in the structure performed much as reported in the database using coupon tests. This also appeared to be true in compression failures (predominantly static) despite complications in compression coupon testing. Failure modes in the beams became complex as materials with improved performance were used, often including adhesive failure at the web/flange connection. Of particular note is Fig. 7, where the web material must perform in fatigue at the same strain level as does the flange (this would also be true of bonded

skins). If the web material has a lower strain for failure in tensile fatigue, then it will fail adjacent to the flange before the flange fails, and may produce structural failure of the beam. (In fact, in a typical laminate, the $\pm 45^\circ$ [or other off-axis] layers will generally crack prior to 0° ply failure, and this will reduce the laminate stiffness in an approximately predictable manner [1].)

4. PREDICTING SERVICE LIFETIMES

Sutherland and Mandell [5] and Sutherland [11] have demonstrated use of the MSU/DOE database to predict service lifetimes for wind turbine blades. As the high-cycle portion of the database is primarily composed of data obtained from specialized material coupons (tested using unidirectional specimens in the longitudinal direction at high frequency [1]), the requisite Goodman diagram is constructed using normalized coupon data. It is then de-normalized to typical industrial laminates for the analysis of service lifetimes. The procedures described in this reference should be used to ensure the blade material used in the construction of the wind turbine is the same as the blade material being analyzed. The analysis is based on material coupons that perform close to the "good" line in Fig. 1 and will be non-conservative for "poor" laminates.

Of particular significance in comparing predictions between the MSU/DOE and the European database is a significant change in the form of the Goodman diagram. In particular, the MSU/DOE database [Fig. 8(a)] yields a highly non-symmetric diagram with a strain to failure of 2.7% and 1.5% for tensile and compressive strains, respectively [5]. This ratio of the tensile and compressive failure strains of 1.80 is significantly different from the European database which has a ratio of 1.33 [Fig. 8(b)]. Namely, the European database yields an approximately symmetric (about the zero mean-stress axis) Goodman diagram with strain-to-failure of 2.58 and 1.94 in tension and compression, respectively [2]. A symmetric diagram implies that there are only small differences between tensile and compressive failures. When the two are compared on a normalized basis, the tensile-failure sides of the diagrams (R values between 0 and 1), are in general agreement. However, on the compressive side, there are significant differences in strains to failure. When de-normalized, the differences are even more apparent. Using the WISPER-protocol U.S. wind farm load spectrum, the predicted service lifetimes for tensile failure were comparable (44.9 to 67.5 years based on the MSU/DOE and the FACT databases, respectively). However, for compressive failures, the predictions differed by approximately a factor of 5 (23.5 to 136 years, respectively). The differences between the two databases may reflect differences in compressive test methods as well as different materials [1,5]. Detailed comparisons of fatigue data from "identical" materials will be required to sort out the differences in the two databases.

Conditions to produce matrix cracking are also reported in the DOE/MSU database [1]. The fatigue behavior of unidirectional materials loaded transverse to the fiber direction has been determined out to 10^8 cycles at various R-values using similar high frequency test techniques to those used for the longitudinal Goodman Diagram in Fig. 8(a). Fig. 8(c) shows much lower strains in

tension and a strong shift to improved performance in compression for initial damage (matrix cracking).

5. CONCLUSIONS

The DOE/MSU database provides static and fatigue data for potential blade materials for which the main parameters of fiber content, fabric architecture, and percent 0° and $\pm 45^\circ$ material have been systematically varied. The data indicate a trend to poor tensile fatigue performance at higher fiber volume fractions (and in structural details

where fibers are locally crowded together) for fabrics with tight strands. Triaxial fabrics with 0° and $\pm 45^\circ$ plies stitched together perform poorly in tensile fatigue even at low fiber contents. Substructural element testing has validated the application of the database for structural design. Blade service lifetime predictions show sensitivity to differences between DOE/MSU and FACT databases in the compression portion of the Goodman diagram.

REFERENCES

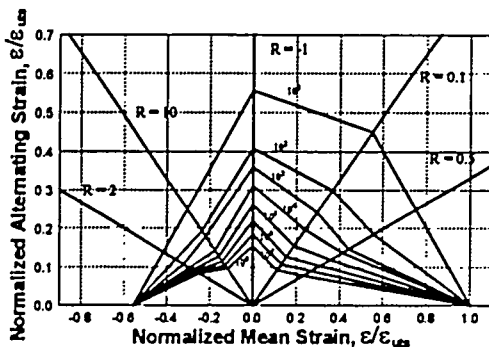


Fig. 8(a). Normalized Goodman Diagram for Unidirectional Material Tested in the Longitudinal Direction (DOE/MSU Database).

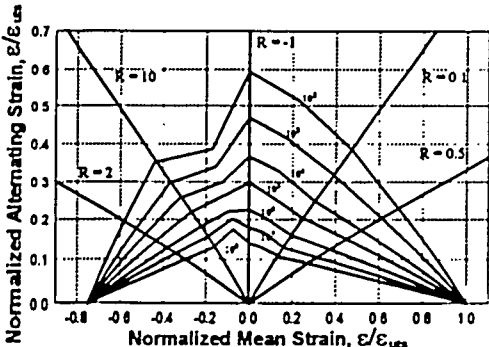


Fig. 8(b). Normalized Goodman Diagram Based on FACT Database.

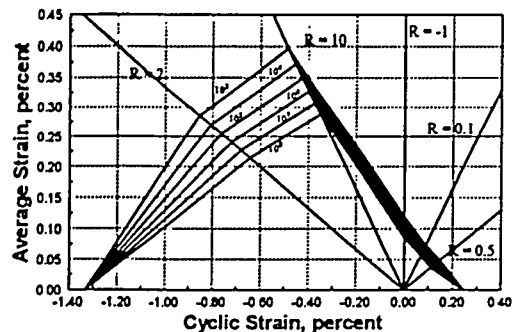


Fig. 8(c). Unnormalized Goodman Diagram for Unidirectional Material Tested in the Transverse Direction (DOE/MSU Database).

Figure 8. Goodman Diagrams, from the DOE/MSU Database (a and c) [1] and the FACT Database (b) [2].

- [1] J.F. Mandell and D.D. Samborsky, *DOE/MSU Composite Materials Fatigue Database: Test Methods, Materials, and Analysis*, SAND97-3002, Sandia National Laboratories, Albuquerque, NM (1997).
- [2] B.J. De Smet and P.W. Bach, *Database FACT: Fatigue of Composite for Wind Turbines*, ECN-C-94-045, ECN, Petten, (1994).
- [3] J.F. Mandell, R.M. Reed, and D.D. Samborsky, *Fatigue of Fiberglass Wind Turbine Blade Materials*, SAND92-7005, Sandia National Laboratories, Albuquerque, NM (1992).
- [4] D.D. Samborsky and J.F. Mandell, *Wind Energy: Wind Energy Week*, ASME/API, 1996, 46.
- [5] H.J. Sutherland and J.F. Mandell, *Wind Energy: Wind Energy Week*, ASME/APT, 1996, 85.
- [6] D.E. Combs and D.D. Samborsky, *Wind Energy-1995*, W.D. Musial, S.M. Hock, and D.E. Berg, eds., SED-Vol. 6, ASME, 1995, 99.
- [7] D.S. Cairns, J.F. Mandell, M.E. Scott, and J.Z. Macagnano, *1996 Wind Energy Symposium*, AIAA/ASME, W. Musial and D.E. Berg, eds., 1997, 197.
- [8] J.F. Mandell, D.D. Samborsky, M.E. Scott, and D.S. Cairns, *1998 ASME Wind Energy Symposium*, W. Musial and D.E. Berg, eds., 1998, 323.
- [9] D.D. Samborsky, J.F. Mandell, and D.S. Cairns, *1999 ASME Wind Energy Symposium*, AIAA/ASME, W. Musial and D.E. Berg, eds., 1999, 32.
- [10] J.F. Mandell, D.D. Samborsky, D.W. Combs, M.E. Scott, and D.S. Cairns, *Fatigue of Composite Material Beam Elements Representative of Wind Turbine Blade Substructure*, NREL/SR-500-24379, National Renewable Energy Laboratory, Golden, CO (1998).
- [11] H.J. Sutherland, *On the Fatigue Analysis of Wind Turbines*, Sandia National Laboratories, Albuquerque, NM (in press).
- [12] J.F. Mandell, "Fatigue Behavior of Short Fiber Composite Materials," *The Fatigue Behavior of Composite Materials*, K.L. Reifsnider, ed., Elsevier, 1991, 232.
- [13] D.R.V. Van Delft, G.D. de Winkel, and P.A. Josses, *1997 ASME Wind Energy Symposium*, AIAA/ASME, W. Musial and D.E. Berg, eds., 1997, 180.